TOWARDS A SET OF DESIGN RECOMMENDATIONS FOR PRESSURE RELIEF DEVICES ON-BOARD HYDROGEN VEHICLES

Yates, D.[1], Makarov, D.[1] and Molkov, V. [1]
[1] HYSAFER, ULSTER UNIVERSITY, SHORE ROAD, NEWTONABBEY, BT37 0QB, YATES-D@EMAIL.ULSTER.AC.UK

ABSTRACT

Commercial use of hydrogen on-board fuel cell vehicles necessitates the compression of hydrogen gas up to 700 bar, raising unique safety challenges. Potential hazards to be addressed include jet fires from high-pressure hydrogen on-board storage. Previous studies investigated effects of jet fires that occur when pressure relief devices (PRDs) on hydrogen fuel cell vehicles activate. This investigation examines plane jets' axis switching and flame length, accounting for compressibility effects and turbulent combustion near the point of release. Comparison with experimental data and previous plane jet simulation results reveal that combustion process does not affect flow dynamics in compressible region of jet flow. Furthermore, a theoretical design of a variable aperture pressure relief device is examined, which would enable the blow-down time to be minimized while reducing deterministic separation distances is examined using Computational Fluid Dynamics (CFD) techniques. Design recommendations are suggested for a novel PRD design.

Symbol	Parameter
A	Area
AR	Aspect ratio
$c_{b,2}$	Spalart-Allmaras model constant
C_{μ}	Model constant
D	Turbulent destruction term
Δx	Valve displacement
ε	Turbulent dissipation rate
F	Force
I	Turbulent intensity
k	Turbulent kinetic energy
l	Turbulent length scale
$\tilde{\upsilon}$	Modified turbulent viscosity
P	Turbulent production term
σ_{υ}	Viscous stress tensor
T	Temperature
u_{avg}	Average flow velocity
u'	Fluctuating velocity

1.0 INTRODUCTION

Current industrial use of carbon-based fuels for energy has led to impacts on natural and human systems on all continents and across all oceans [1]. Unless the global economy transitions posthaste to a more sustainable energy paradigm, consequences of climate change will manifest with greater frequency and severity. Hydrogen has potential to serve as an alternative energy carrier in a future renewable energy economy if sustainable sources of energy supplant the use of fossil fuels, but despite this promise, there are some safety concerns associated with use of hydrogen as an energy carrier [2].

One way in which hydrogen automobiles store fuel is in compressed gas form at pressures up to 700 bar, allowing them to achieve driving ranges comparable to existing petrol vehicles [3]. In the event of a fire accident involving a hydrogen car, a tank failure due to overpressure would cause catastrophic damage to the surroundings [4]. To prevent this, tanks are outfitted with a pressure relief device (PRD). Unfortunately, current standards and regulations do not have safety requirements for PRDs, silently implying that hydrogen tank should be vented as quickly as possible. As a result the present design of PRDs may have a nozzle on the order of 5 mm [3], which, when activated, would liberate hydrogen at a high flow rate that, when ignited, would extend of tens of meters and would pose a hazard to emergency responders and others in the vicinity [5].

Tamura and colleagues [6] examined the ignition and spread of fires between hydrogen automobiles in a closed transportation container and associated activation of PRDs on the storage tanks. They showed that the PRD on the ignited car activated within an hour of ignition of the car, leading to both flame spread between vehicles and PRD activation of adjacent vehicles. It was suggested that PRD activation of one vehicle could lead to activation of PRDs in adjacent vehicles, posing a hazard for hydrogen cars parked in close proximity to one another, unless the hydrogen was released in a more controlled manner.

Mogi and Horiguchi [7] examined high-pressure hydrogen jets issuing through round and plane nozzles of equivalent diameter 1 mm. They gave a simple power relationship between inlet pressure and flame length and width for their round nozzle conditions, and further demonstrated that the use of a rectangular nozzle instead of a plane nozzle would reduce the flame length substantially. Specifically, a plane nozzle of aspect ratio (AR) 12.8 would reduce the flame length from 2.5 m to 1.0 m compared to a round nozzle of equivalent cross-sectional area. The nozzle asymmetry also gives rise to a phenomenon called axis switching [8], wherein the cross-section of an asymmetric jet evolves in such a way that after a certain distance the minor and major axes exchange locations along the jet. The switchover location is unclear and varies between different aspect and pressure ratios, with supersonic jets switching occurring earlier and more strongly than subsonic.

Kalghatgi [9] suggested that the flame will stabilize at the outer edge of the turbulent jet mixing layer, at a point where the turbulent burning velocity equals the local flow velocity. The liftoff height was measured for converging-diverging nozzles with diameters ranging from 1.08-6.1 mm and exit velocities from 500-2000 m/s. The liftoff heights collapsed onto a single curve independent of nozzle diameter, reaching 5-6 mm for a sonic exit velocity of 2000 m/s. Xu and co-workers used two-domain approach to model a highly underexpanded axisymmetric non-reacting jet [10]. Near to the nozzle, a RANS simulation of the shock structures was carried out to provide the input boundary for a second domain where, farther from the nozzle, a Large Eddy Simulation (LES) approach was used to examine subsonic jet development. Makarov and Molkov [11] used this two-domain approach to simulate the fires from Mogi's investigation using the k-epsilon turbulence model and the Eddy Breakup model to simulate turbulence-chemistry interaction in the far field domain, while combustion was switched off in the near-nozzle region. The Eddy Breakup model uses one-step combustion and models the interaction between turbulence and chemical kinetics.

The present investigation extends the aforementioned work of Makarov and Molkov, looking at the effect of including near-nozzle combustion and a different turbulence model. Also, a theoretical PRD design is examined to better control the flow rate of hydrogen in PRD activations. Results culminate in design recommendations for PRDs that improve the protection of automobile occupants and emergency responders from hydrogen releases.

2.0 MODEL AND SIMULATION APPROACH: PLANE JET FIRES

2.1 Plane jet calculation domains

Three dimensional continuity, momentum, and species conservation equations were solved in this investigation. The compressible form of the ideal gas law was used. The range of length scales pertinent to the investigation of high-pressure hydrogen releases poses a modelling challenge as different flow features need to be realized at each scale simultaneously in order for the simulation to proceed. In order to reconcile these disparate scales, a two-stage modelling approach was employed [10],[11], with separate calculation domains near the nozzle and further downstream.

In this study the near-to-the-nozzle and far-from-the-nozzle calculation domains were used as in [11] to minimize numerical error in results comparison. In the first domain, hydrogen at 40 MPa was introduced upstream of a nozzle of 1 mm diameter or equivalent in the case of the AR=12.8 plane nozzle. This domain extended to x=9 cm and had an interior interface, which provided the boundary between the near and far fields at x=3 cm. The outflow boundary of the first domain was sufficiently remote from the interior interface to minimize the effects of the enforced pressure-outflow boundary condition. The Spalart-Allmaras turbulence model [12] was used in this domain to resolve the shock structures and near-nozzle flow features based on the findings of Menon and Skews [13] for these flows, along with laminar finite-rate chemistry and the ideal gas law equation of state [14].

The second domain took a pressure-inflow boundary condition from the interior interface of the first domain, where pressures, velocities, and mass fractions were written as inflow conditions for the second domain. The second domain extends 5 m downstream. The realizable k-epsilon model [14] was used in this domain with the Eddy-Dissipation concept for turbulence-chemistry interaction [15].

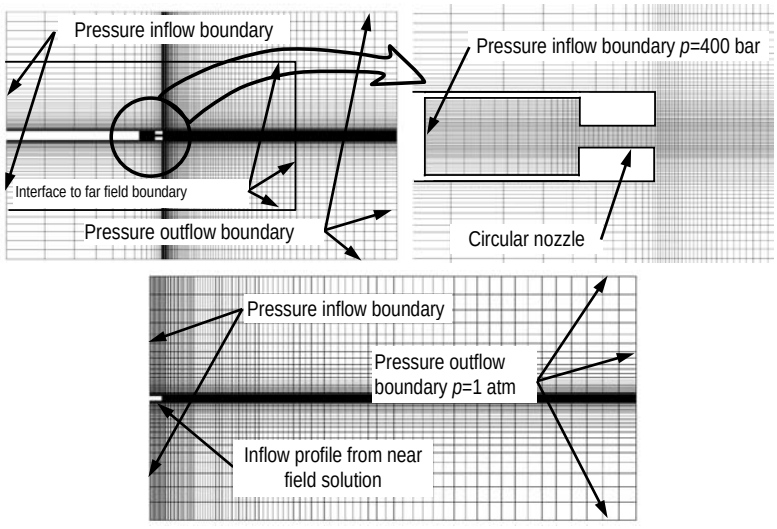

Figure 1. 3D calculation domain for jet fire investigations [11]. Top left: near field, full domain. Top right: near field, near nozzle. Bottom: far field domain.

2.2 Turbulence model interpolation for plane jet fires

Because different turbulence models were used based on the pertinence of different flow features that needed to be realized in each of the two domains (Spalart-Almaras in the near field and realizable k-

epsilon model in the far-field), a way to reconcile the different turbulence model parameters was necessary. The Spalart-Allmaras turbulence model is a single transport equation for modified turbulent viscosity $\tilde{\upsilon}$,

$$D\tilde{\upsilon} / Dx_1 = P - D + 1/\sigma_v[\nabla \cdot \{(\upsilon + \tilde{\upsilon})\nabla \upsilon\} + c_{b,2}\tilde{\upsilon}^2], \quad (1)$$

which is defined as

$$\tilde{\upsilon} = \sqrt{3/2}u_{avg} Il . \quad (2)$$

The turbulent viscosity production, *P*, destruction, *D*, viscous stress tensor σ_υ, and model constant $c_{b,2}$ are defined in [14]. The mean flow velocity is u_{avg}, turbulent intensity is *I*, and the turbulent length scale is *l*. The fluctuating turbulent velocity is defined as

$$u' = u_{avg} I , \quad (3)$$

and the turbulent kinetic energy is

$$k = 3/2u'^2 . \quad (4)$$

A constant turbulent intensity was assumed exiting from the near field domain, based on the results of Brennan et al. [16]. Constant values of turbulent intensity between 5 and 50% were examined. The turbulent length scale *l* can then be calculated by substitution of equations 3 and 4 into 2.

With the turbulent velocity fluctuation now defined, the k-epsilon model parameters are accessible and can be written into a boundary profile using only the Spalart-Allmaras variables. The turbulence dissipation rate, ε, is defined as

$$\varepsilon = C_\mu^{3/4} k^{3/2} / l , \quad (5)$$

with model constant C_μ = 0.09. These model parameters comprise the inputs for the realizable k-epsilon turbulence model in the far field.

3.0 RESULTS: PLANE JET FIRES

3.1 Flame size and experimental comparison

Flame length was compared with experimental results for model validation of the AR 1 and AR 12.8 case, where temperature cut-off corresponding to visible flame was taken as *T*=1300-1500 K [17], [18], [19]. Different values of constant turbulent intensity across the inter-domain interface ranging from 5% to 50% were tested. A constant turbulent intensity of 10% best matched the experimental results; all other intensities overpredicted the flame length for a variety of higher and lower intensities. The simulated flame length from the round nozzle (AR=1) was 2.7 m (T=1500 K), compared to a measured length of 2.5 m. The simulated flame length from the plane nozzle was 1.2 m, compared to 1.0 m experimentally measured one. The previous approach of Makarov and Molkov [11], where a temperature cut-off *T*=1300 K was used, tended towards smaller flame lengths compared to experiment and present simulations, but all modelled lengths were within 20% of the experimental results. The flame width of the round nozzle was modelled to be 0.3 m, compared to 0.3 m experimentally, and the model plane nozzle flame width was 1.0 m, compared to 0.8 m experimentally. Simulated flame shapes for both round and plane nozzles are given in Figures 2 and 3 in comparison with experimental data and results of Makarov and Molkov. Figure 4 shows flame length as a function of boundary value of turbulent intensity, and flame length results are in table 1.

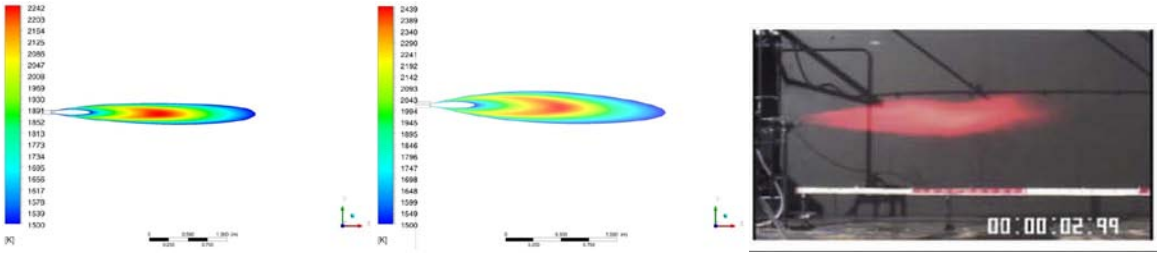

Figure 2. Flame length along centre plane for round nozzle at 40 MPa, T>1500 K. Modelled L_f = 2.7 m (EDC), 2.3 m (EBU), experimental L_f = 2.5m [9].

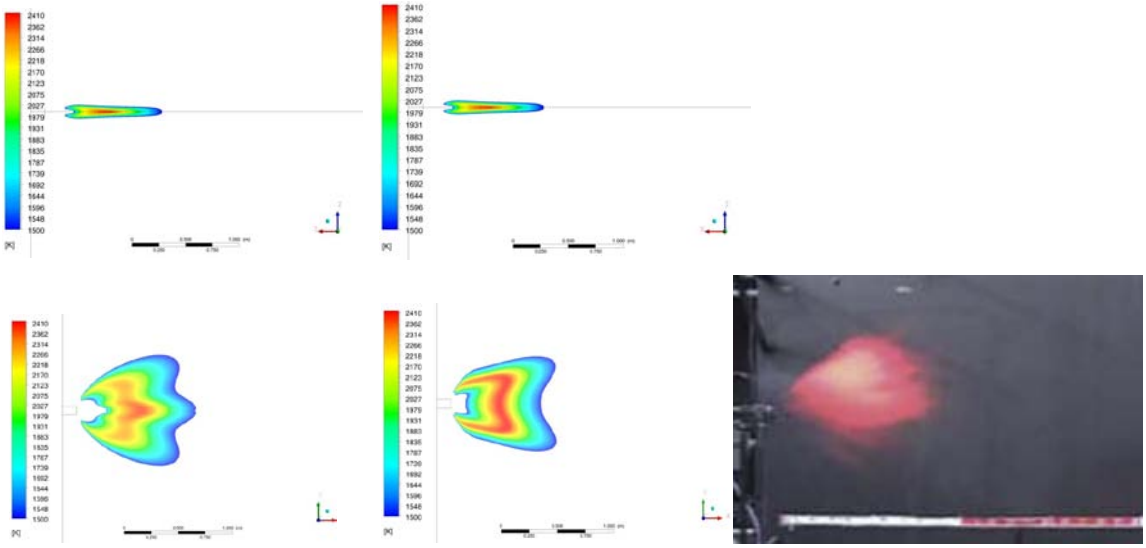

Figure 3. Plane nozzle flame (AR=12.8, 40 MPa): Top: major axis plane, bottom: minor axis plane. From left to right: simulation results, present study, L_f =1.0 m (EDC); simulation results [11], L_f =1.2 m (EBU), experimental L_f = 1.0 m [7].

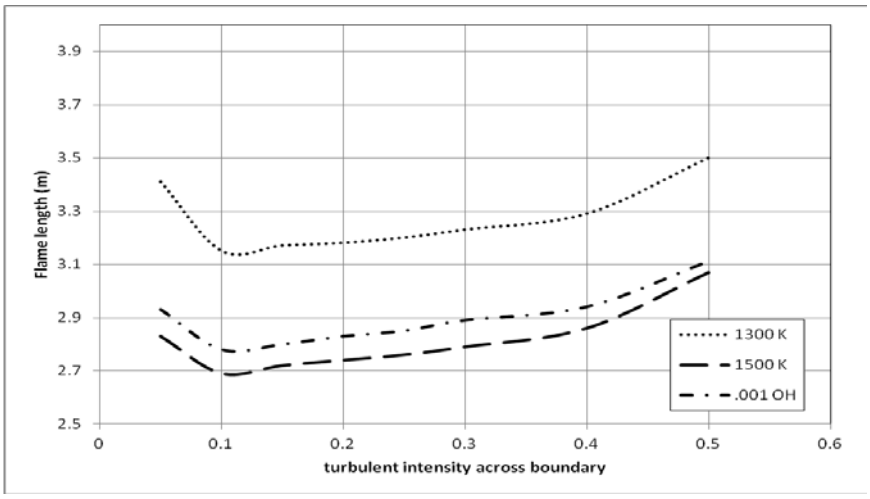

Figure 4. Flame length at different turbulent intensities across the interface

Table 1. Flame length for different nozzles and domain boundary conditions

AR	I	Model	Compressibility	Lf (m)		
				1300 K	1500 K	.001 OH
1	n/a	EBU	incomp	2.50	2.27	n/a
1	0.05	EDC	comp	3.41	2.83	2.93
1	0.1	EDC	comp	3.15	2.69	2.78
1	0.15	EDC	comp	3.17	2.72	2.80
1	0.2	EDC	comp	3.18	2.74	2.83
1	0.25	EDC	comp	3.20	2.76	2.85
1	0.3	EDC	comp	3.23	2.79	2.89
1	0.4	EDC	comp	3.29	2.86	2.94
1	0.5	EDC	comp	3.50	3.07	3.11
12.8	n/a	EBU	incomp	1.18	1.01	n/a
12.8	0.1	EDC	comp	1.38	1.20	1.28
12.8	0.2	EDC	comp	1.34	1.18	0.99

4.2 Near field: axis switching

The hydrogen concentration was examined at different downstream locations on planes normal to the nozzle centreline for rectangular jets. This characterized the axis switching of the jet, which occurred within 0.05 equivalent nozzle diameters (less than the width of one control volume) due to the highly underexpanded nature of the jets (pressure ratio 400). The axis switching data were examined at different stations downstream using hydrogen volume fraction cut-off of 4% and results are presented in Figure 6 and Table 2. Results are compared with the previous results of Makarov and Molkov, who used the k-epsilon model in their near field results.

Axis switching occurred immediately after the nozzle: less than one nozzle diameter downstream, the flame had already expanded further in the minor axis plane than the major. The jet aspect ratio had inverted completely by 25 equivalent nozzle diameters (D_{eff}=1 mm) downstream in the previous investigation, and switched 25% less over the same distance in the present case, but by the time the flow entered the combustion region the axes were completely switched. As a consequence, the flame takes a wider but shorter shape, nearly as wide as it is long. Mogi reported a flame width of 0.8 m for the considered conditions and an AR 12.8 nozzle (in the present numerical investigation the width was simulated as 1.0 m). The orientation of the wide part of the flame issuing through a plane jet is therefore a crucial design consideration for PRDs exploiting this geometry, because the width of the flame is comparable to that along its length. The definition of separation distances, derived for high-temperature flow along the jet axis, may need to be reconsidered in light of the expanded jet width [3].

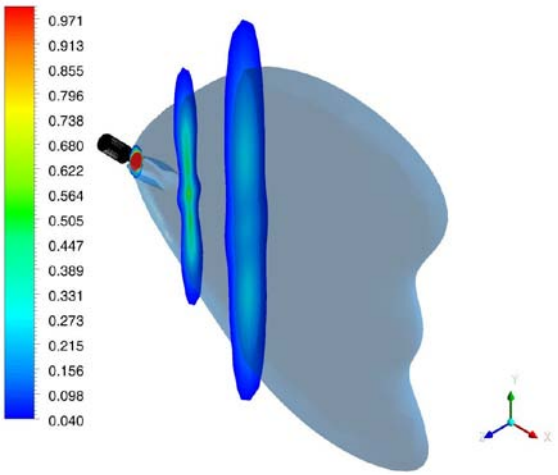

Figure 5. Hydrogen mass fractions in cross-sections normal to the nozzle centreline, x/D = 0.5, 25, 50, with overlay of isocontour of Y_{H2} = 0.11 Major axis of plane nozzle is along jet minor axis plane.

Table 2. Jet aspect ratio at different downstream locations from AR=12.8 nozzle

	S-A		k-epsilon	
x/D	AR	1/AR	AR	1/AR
0.05	0.72	1.38	0.48	2.09
0.5	0.60	1.65	0.57	1.76
5	0.44	2.26	0.33	3.02
25	0.11	8.99	0.08	12.11

5.0 MODEL AND SIMULATION APPROACH TO VARIABLE APERTURE PRESSURE RELIEF DEVICE (VAPRD)

5.1Design goals of a VAPRD

An investigation was undertaken of a hypothetical PRD that would improve blow-down performance over existing designs. Thermally activated PRD (TPRD) designs for on-board storage typically open and stay open for the duration of blow-down when a critical exterior temperature is reached. This means that the flow rate through the TPRD is initially very high but drops with the upstream pressure. When the TPRD opens, the sudden release of air has potential to cause long flames and rapid and catastrophic increases in pressure in interior spaces [3], [20].

Some reclosing PRD designs use a valve seat that lifts off in the direction of flow when a critical pressure is reached, and throttles the flow using a spring-loaded system. In this configuration, the mass flow rate increases with increasing upstream pressure and decreases as the tank blows down, ultimately reaching the reseat pressure at which the flow through the TPRD ceases **[21]**. This is currently recognised as not an inherently safe design as storage tank ruptures in prolonged fire when significant amount of gas under pressure is still within the tank. Fireball and blast wave are generated during tank rupture in a fire.

This investigation sought to examine the features of a variable aperture PRD that, on activation, would throttle the mass flow rate to a constant value though the entire blowdown process. Such a VAPRD would achieve two goals: first, to confine the flame length to a design value by ensuring, for example, a constant pressure in the chamber upstream of the nozzle itself, and second, to ensure that the tank blew down as quickly as possible by increasing the available flow area as the tank pressure dropped. Unlike existing reclosing PRD designs which increase opening area with increasing upstream pressure, this VAPRD would decrease the opening area with increasing upstream pressure.

5.2 Design calculations

The VAPRD design and calculation domain for CFD simulations are presented in Figure 6. The inlet is at the far left, and the throttle mechanism is secured by a compression spring pushing in the direction opposite that of flow. The pressure gradient from the inlet across the throttle exerts a force on the throttle mechanism which is counter-balanced by the spring assembly.

The investigated pressures through the nozzle range as high as 70 MPa, and so there is a departure from ideal gas behaviour that necessitates the use of a real gas model. The Peng-Robinson real gas model was employed for this investigation for its applicability to highly compressed hydrogen [14].

Figure 7 shows the calculation scheme for the considered VAPRD. Assuming that the valve seat is parallel to the throttle slant, the distance h between the throttle and the valve seat is directly related to the valve displacement Δx with the valve seat angle θ, throttle radius r_1, and initial valve seat radius r_2 as constants:

$$h = \min([\cos(\theta)(r_2 - \{\Delta x \tan(\theta) + r_1\}], r_2 - r_1), \tag{6}$$

and the flow area can thus be calculated by the surface of revolution around the symmetry axis

$$A_{throt} = 2\pi h(r_1 + h\cos(\theta)/2), \tag{7}$$

or, non-dimensionalised by the area of the nozzle exit,

$$A_{ratio} = [8h(r_1 + h\cos(\theta)/2)]/D^2. \tag{8}$$

For compressible flow through a round orifice, the mass flow rate is for sonic flow [3]

$$\dot{m} = C_d A \sqrt{\gamma \rho_0 P_0 \left(\frac{2}{\gamma+1}\right)^{\frac{\gamma+1}{\gamma-1}}} \tag{9}$$

where C_d is the discharge coefficient, A the exit area, γ the specific heat ratio, ρ_0 the inlet density, and P_0 the upstream pressure. The orifice in this case is throttled and the flow is dependent on the throttling area rather than the nozzle exit area, which has an unknown and possibly variable discharge characteristics, so the mass flow rate dependence on pressure and throttle displacement is more complex and will be investigated using CFD.

5.3 Calculation domain: VAPRD

During tank blow-down, the pressure in the tank drops from a peak of 70 MPa to ambient pressure. For a PRD of 1 mm diameter, an investigation was carried out to see if the flame length could be confined to a small constant value during the blow-down of the tank. By keeping a constant mass flow rate, the blow-down time could be minimized and the flame length (separation distance) would remain the same at all stages of blow-down.

A nozzle diameter of 1 mm was investigated with a desired constant flame length of 1 m across a range of pressures from 70 MPa to 12.5 MPa. This flame length corresponds to a mass flow rate of 3.8 g/s or a pressure upstream of the nozzle of 10 MPa. A domain was designed where the flow into the chamber upstream of the nozzle was throttled, shown in Figure 6. This throttle is beside a slanted wall, varying the size of the interstitial aperture in order to maintain a constant nozzle mass flow rate. The forces on the throttle assembly are calculated to examine the viability of a spring assembly that would move the throttle in such a way as would preserve a constant mass flow rate.

A 2D calculation domain, axisymmetric about the x-axis, was employed for simplicity. As in the plane jet investigation, the standard continuity, momentum, energy, and species conservation equations were employed alongside the Spalart-Allmaras turbulence model with laminar finite-rate chemistry [14]. For each of several fixed throttle locations, the inlet pressure was varied to find the point at which the mass flow rate was a constant 3.8 g/s.

6.0 RESULTS: DESIGN ATTRIBUTES OF A VAPRD

6.1 Example valve performance

Six constant valve displacements were examined across several inlet pressures in order to ascertain the correspondence between inlet pressure and valve displacement leading to the desired mass flow rate. For each constant valve displacement, a linear relationship between pressure and mass flow rate was observed. These trendlines are plotted in Figure 8.

Figure 9 shows upstream pressure and force exerted on the throttle assembly as a function of valve displacement corresponding to constant mass flow rate 3.8 g/s. The force on the throttle assembly was also examined to ascertain the characteristics of a hypothetical spring that would keep the mass flow rate constant. A linear spring assembly was assumed with a constant spring coefficient. Over the investigated range of valve displacements and pressures, a linear trendline had an R^2 value of 0.93, indicating a strong correlation. The slope of this trendline was 57.8 N/mm.

A representative fuel cell vehicle, the Hyundai ix35, has a tank volume of 114 L [22]. Given an initial pressure of 70 MPa, the unrestrained hydrogen mass flow rate through the PRD with 1 mm diameter gives a mass flow rate of 118.6 g/s, flame length of 3.3 m [23] and blowdown time to 0.1 MPa overpressure about 25 minutes. By throttling the mass flow to a constant 3.8 g/s, the flame length can be reduced by more than 3 times to just 1 m. As a consequence, the blow-down time would increase by an additional 10 minutes compared to the unrestrained blow-down, for a total blow-down time of 35 minutes.

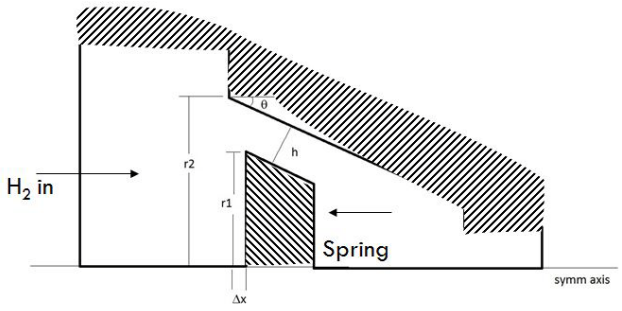

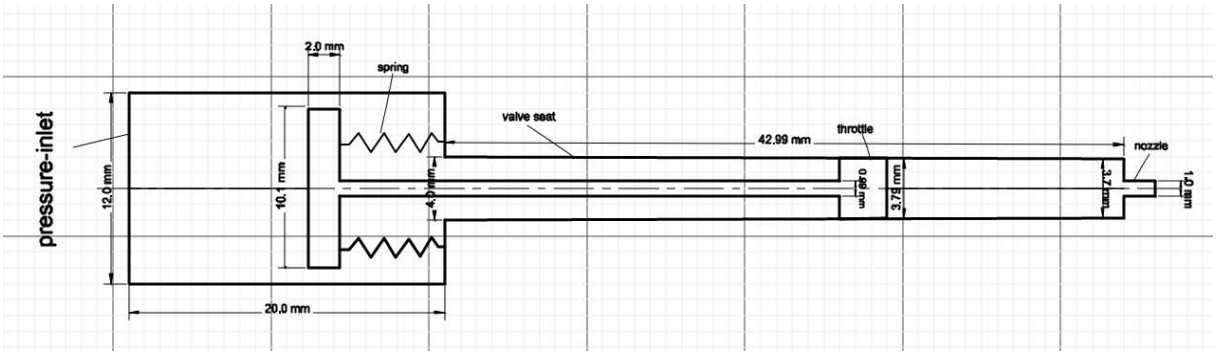

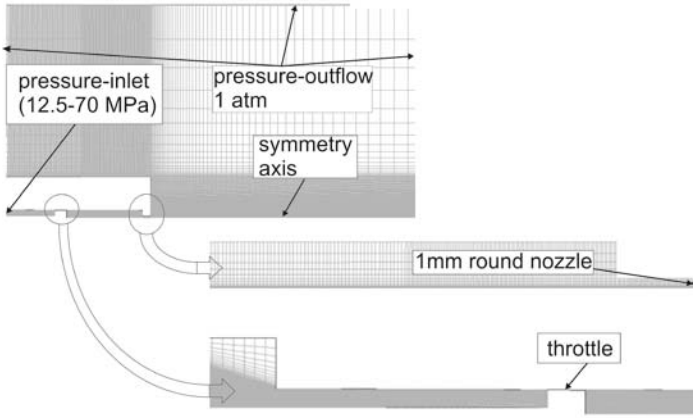

Figure 6. VAPRD design parameters (top); nozzle schematic (centre); and 2D axisymmetric calculation domain for VAPRD investigation: full domain, nozzle chamber, and throttle (bottom).

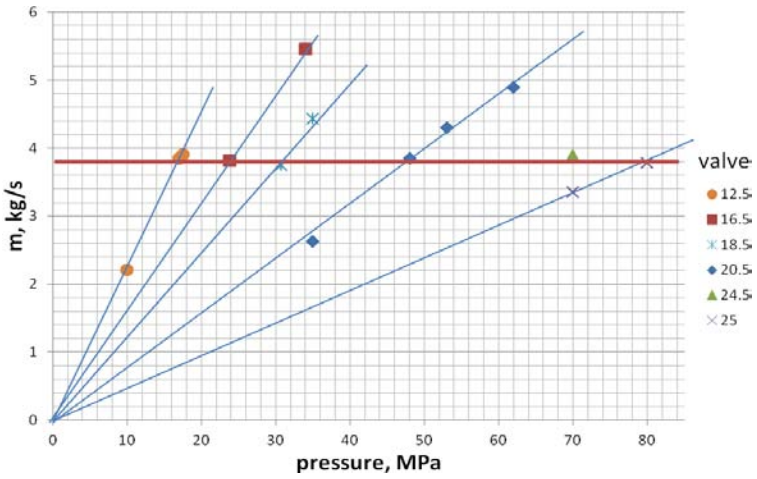

Figure 7. Calculated mass flow rates at different valve locations leading to constant pressure

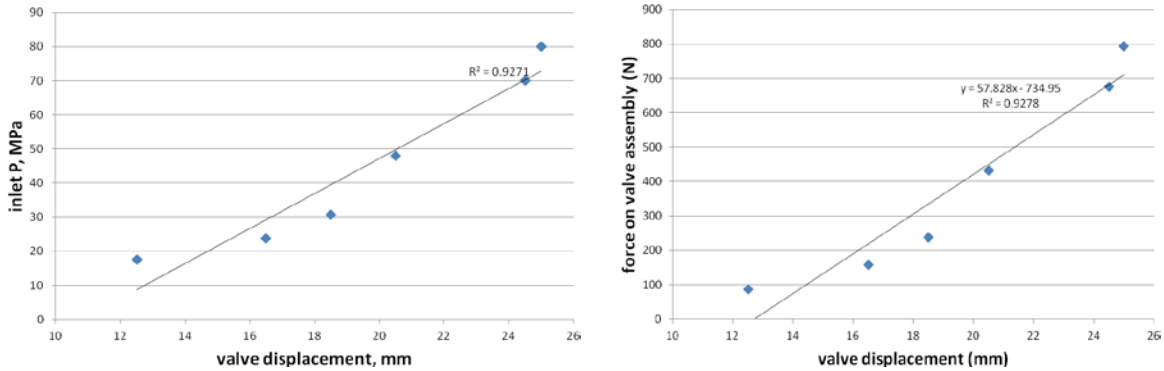

Figure 8. Inlet pressure, force on valve v. displacement

Table 3. Simulation results for VAPRD (note: some forces omitted for simulations that didn't arrive at target mass flow rate).

Δx (mm)	A_{ratio}	P_{inlet} (MPa)	F_{valve} (N)	m (g/s)
12.5	.869	10	-	2.2
12.5	.869	17	86.5	3.85
12.5	.869	17.5	-	3.9
16.5	.652	34	224.7	5.46
16.5	.652	23.8	157.9	3.82
18.5	.543	35	-	4.4
18.5	.543	30.7	238.4	3.75
20.5	.436	62	-	4.9
20.5	.436	53	-	4.3
20.5	.436	48	432.4	3.85
20.5	.436	35	320.1	2.63
24.5	22.1	70	676.4	3.89
25	19.4	70	694.4	3.35
25	19.4	80	793.5	3.79

6.0 CONCLUSIONS: DESIGN RECOMMENDATIONS FOR ON-BOARD HYDROGEN STORAGE

The present PRD designs for use on-board hydrogen automobiles have the potential to cause dangerous hydrogen fires and cause damage to life and property if the release of hydrogen is not controlled. Understanding some of the flow features of hydrogen jets can aid in the design of PRDs that will have shorter length of jet fires and pose a lesser risk to occupants and emergency personnel while still evacuating the tank in sufficient time to avoid catastrophic failure.

The investigation of hydrogen plane jet fires of Makarov and Molkov was extended, employing finite-rate chemistry and the Spalart-Allmaras turbulence model to better resolve the shock structures in the near-to-nozzle field. Bridging of the solutions in the near and far fields was performed assuming a constant value of turbulence intensity I = 10% at the domain interface. The modelling of combustion in the near-to-the-nozzle field demonstrated that modelled chemical reactions there do not affect jet dynamics, as most of the combustion occurs further downstream in the second calculation domain. The axis switching of the plane jet began almost immediately downstream of the nozzle and within 25 equivalent nozzle diameters the jet had switched completely. The plane jets were shown to reduce flame length by 2.5 times at the same inlet pressure and nozzle cross-section area, a finding corroborated by experiment. If a plane nozzle is to be used in a PRD, however, it was noted that the orientation of the nozzle is a crucial design consideration because the flame width is of the same order as the length, with potential ramifications for the tank and wheels.

A potential design for a variable aperture PRD was explored with the goal of developing a throttle that decreases the allowable flow area with increasing upstream pressure (rather than increasing the flow area with increasing pressure, as in most current designs of reclosing PRDs.) Different combinations of valve displacement and inlet pressure leading to a constant mass flow rate (3.8 g/s) that would confine a flame length to 1m through a 1 mm diameter nozzle were determined. It was observed that for fixed throttles, the inlet pressure and mass flow rate were nearly linearly related. The force on the throttle was proportional to its displacement for fixed mass flow rate, indicating that a simple spring system could theoretically be used to hold the throttle in place. Specifications of the spring system were suggested, and it was noted that such a throttling action would increase blow-down time by about ten minutes resulting in total blowdown time of 35 min that would require additional thermal protection of storage tanks.

REFERENCES

1.C. B. Field, *Climate Change 2014: Impacts, Adaptation, and Vulnerability: Summary for Policymakers*. 2014.

2.B. P. Xu and J. X. Wen, "Numerical study of spontaneous ignition in pressurized hydrogen release through a length of tube with local contraction," *Int. J. Hydrog. Energy*, vol. 37, no. 22, pp. 17571–17579, Nov. 2012.

3.V. Molkov, "Fundamentals of Hydrogen Safety Engineering." Bookboon, 2012.

4.R. Zalosh, "Blast waves and fireballs generated by hydrogen fuel tank rupture during fire exposure," Firexplo, Wellesley, MA, USA.

5.F. Verbecke, "Formation and Combustion of Non-Uniform Hydrogen-Air Mixtures," PhD, University of Ulster, Jordanstown, 2009.

6. Y. Tamura, M. Takabayashi, and M. Takeuchi, "The spread of fire from adjoining vehicles to a hydrogen fuel cell vehicle," *Int. J. Hydrog. Energy*, vol. 39, no. 11, pp. 6169–6175, Apr. 2014.

7.T. Mogi and S. Horiguchi, "Experimental study on the hazards of high-pressure hydrogen jet diffusion flames," *J. Loss Prev. Process Ind.*, vol. 22, no. 1, pp. 45–51, Jan. 2009.

8.K. Zaman, "Axis switching and spreading of an asymmetric jet: the role of coherent structure dynamics," *J. Fluid Mech.*, vol. 316, pp. 1–27, 1996.

9. G. Kalghatgi, "Liftoff heights and visible flame lengths of vertical turbulent jet diffusion flames in still air," *Combust. Sci. Technol.*, vol. 41, pp. 17–29, 1984.

10.B. P. Xu, L. EL Hima, J. X. Wen, and V. H. Y. Tam, "Numerical study of spontaneous ignition of pressurized hydrogen release into air," *Int. J. Hydrog. Energy*, vol. 34, no. 14, pp. 5954–5960, Jul. 2009.

11.D. Makarov and V. Molkov, "Plane hydrogen jets," *Int. J. Hydrog. Energy*. 2009: vol. 38, no. 19: pp. 8068-8083.

12.P. R. Spalart and S. R. Allmaras, "A one-equation turbulence model for aerodynamic flows," *Rech. Aerosp.*, vol. No.1, pp. 2544–2553, 1994.

13.N. Menon and B. W. Skews, "Shock wave configurations and flow structures in non-axisymmetric underexpanded sonic jets," *Shock Waves*, vol. 20, no. 3, pp. 175–190, May 2010.

14."ANSYS FLUENT 12.0 Theory Guide - 4.3.1 Overview." [Online]. Available: http://www.sharcnet.ca/Software/Fluent12/html/th/node49.htm. [Accessed: 26-Jul-2013].

15.B. F. Magnussen, "The eddy dissipation concept a bridge between science and technology," in *ECCOMAS thematic conference on computational combustion*, 2005, pp. 21–24.

16.S. L. Brennan, D. V. Makarov, and V. Molkov, "LES of high pressure hydrogen jet fire," *J. Loss Prev. Process Ind.*, vol. 22, no. 3, pp. 353–359, May 2009.

17.P. B. Sunderland, B. J. Mendelson, Z.-G. Yuan, and D. L. Urban, "Shapes of buoyant and nonbuoyant laminar jet diffusion flames," *Combust. Flame*, vol. 116, no. 3, pp. 376–386, 1999.

18.F. G. Roper, "The prediction of laminar jet diffusion flame sizes: Part I. Theoretical model," *Combust. Flame*, vol. 29, pp. 219–226, 1977.

19.J. LaChance, "Risk-informed separation distances for hydrogen refueling stations," *Int. J. Hydrog. Energy*, vol. 34, no. 14, pp. 5838–5845, Jul. 2009.

20.S. Brennan and V. Molkov, "Safety assessment of unignited hydrogen discharge from onboard storage in garages with low levels of natural ventilation," *Int. J. Hydrog. Energy*, vol. 38, no. 19, pp. 8159–8166, 2013.

21.M. Malek, *Pressure Relief Devices: ASME and API Code Simplified*. New York: McGraw-Hill, 2006.

22."Green Car Congress: Five Hyundai ix35 Fuel Cell vehicles joining London hydrogen project." [Online]. Available: http://www.greencarcongress.com/2013/07/ix35-20130721.html. [Accessed: 30-Mar-2015].

23."H2FC European Infrastructure." [Online]. Available: http://h2fc.eu/portal. [Accessed: 30-Mar-2015].